The Role of Turbulence in Darrieus-Landau Instability

G. Troiani[1], F. Creta[2], P. E. Lapenna[2], R. Lamioni[2]

[1] ENEA C.R. Casaccia, Rome, Italy
[2] Dept. of Mechanical and Aerospace Eng., University of Rome "La Sapienza", Italy

Abstract
Experimental propane/air Bunsen flame at atmospheric pressure are investigated in the context of Darrieus-Landau (DL) instability. Results from asymptotic theory are utilized in order to estimate the non-dimensional critical length scale $\delta_c = L_D/\lambda_c$ (L_D the flame thickness and λ_c the critical length scale). The non-dimensional flame thickness $\delta = L_D/L$ is varied either by varying the equivalence ratio, which acts on L_D, or by adopting a different Bunsen diameter L. Two Bunsen diameters are chosen so that unstable conditions are met for the larger diameter while stable conditions, $\delta > \delta_c$, are consistently met for the smaller diameter. Results confirm the dichotomic behavior (absence or presence of DL instability) of flame morphology with respect to variations of the parameter $\delta = L_D/L$. It is shown that for the smaller diameter curvature skewness, which is only mildly negative, seems to be insensitive to variations of equivalence ratio. On the other hand, for the larger diameter the skewness becomes abruptly negative and highly sensitive to variations of equivalence ratio. Moreover the abrupt change in skewness is most evident at the lowest bulk Reynolds number, which is considered laminar. Turbulence intensity will play a role in mitigating such effect. We monitor also the global consumption speed and we observe two different regimes of turbulent propagation. Results suggest that the presence of DL-induced flame corrugation can more than double the turbulent propagation speed at a given Reynolds number and mixture composition.

Introduction
A central topic in combustion processes is the prevision to which extent the surface wrinkling proceeds, since the more intense the wrinkling is, the higher the reactant mass flow rate results, increasing the so called turbulent flame speed. Apart from its importance in industrial applications, it is also a scientific challenge due to the multiscale nature of the interaction between chemistry and turbulence. In this context, the presence of intrinsic Darrieus-Landau hydrodynamic instability was recognized as an important factor influencing the propagating characteristics of flames [1]. The long wavelength nature of DL instability makes it particularly important in large scale combustion devices where it is expected to be ubiquitous. A number of experimental studies were performed [2, 3, 4, 5, 6, 7, 8] to emphasize the role of DL instability in the wrinkled flamelet regime.
Recently a series of numerical studies were performed by Creta and Matalon [9, 10, 11, 12], which focused on the systematic derivation of scaling laws for the turbulent flame speed ST in the wrinkled flamelet regime with particular attention to the role of DL instability. The main result of such studies is the identification and description of two very distinct turbulent modes of flame propagation, characterized by the presence or absence of DL instability. The corresponding laminar scenario is well known [13, 14], with a planar flame transitioning, upon onset of DL instability, to a typical large scale cusp-like corrugated conformation steadily propagating at a speed substantially greater than the unstretched laminar flame speed S_L . It was found that in a turbulent scenario a similar dichotomy persists [15]. In particular, a planar flame that is stable in the laminar regime will remain statistically planar, defining a subcritical turbulent mode of propagation, in which turbulence-driven wrinkling is dominant and DL effects absent. A corrugated flame, for which the planar conformation is unstable, in the presence of turbulence will exhibit a more complex flame brush with sharp cusps protruding into the burnt mixture with an asymmetric curvature distribution, thus defining a supercritical turbulent mode in which DL effects are dominant. In addition, for higher intensity turbulence, the effect of DL instability is found to be shadowed and ultimately completely overpowered by the advective effect of turbulence [9, 12, 15].
In this work we face with three distinct questions, namely: first, unambiguously establish the presence or absence of a DL-induced flame morphology on a turbulent premixed flame, given the operating conditions and the fuel type; second, quantify the effect of the intensity of the DL instability on the flame morphology and propagation and third, investigate whether the DL-induced effects are mitigated or even suppressed as

the intensity of the turbulence increases. To this purpose, we perform a series of experiments on propane-air, atmospheric pressure Bunsen flames at different equivalence ratios and different Reynolds numbers. We utilize two distinct Bunsen diameters which are chosen to be respectively above and below the estimated cutoff wavelength in the range of compositions used, i.e. promote or prevent instabilities.
As results of our study, we identify the stability limits for the flame in such a way that DL instability can be induced or suppressed at will. We then identify the skewness of the flame curvature distribution as an unambiguous marker for DL-induced effects on the turbulent flame. We also measure the turbulent propagation speed and assess the effect of the intensity of the DL instability and of the incident turbulence.

Stability Limits
Results from the linear stability analysis of a premixed planar flame can be employed to estimate the conditions for which DL instability is promoted. Asymptotic dispersion relations were rigorously derived under the deficient reactant assumption [16, 17, 18]. Such relations, expressing the growth rate ω(k) of a perturbation of transverse wavenumber k = 2π/λ, with λ the perturbation wavelength, are usually cast in the form of a series expansion in powers of k, truncated so as to include a linear term expressing the DL hydrodynamic instability and a quadratic stabilizing term due to diffusive effects. In particular Ref.[17] yields a general non linear hydrodynamic model in which the flame is a gasdynamic discontinuity between the fresh and burnt mixture, propagating at a flame speed $S_f = S_{0L} - \Lambda K$, where $K = S_{0L}\,\kappa + K_S$ is the flame stretch rate inclusive of the effect of curvature κ and hydrodynamic strain K_S and Λ is the Markstein length. Given the unit normal **n** to the flame, directed towards the burnt gases, then $\kappa = -\nabla\cdot\mathbf{n}$ and $Ks = -\mathbf{n}\cdot\mathbf{E}\cdot\mathbf{n}$, with **E** the rate of strain tensor. A closed form relation expressing $\Lambda / L_D = M$, where M is known as the Markstein number, can be rigorously derived from a generalized version of the hydrodynamic model [19] in terms of operative parameters such as σ (unburned to burned density ratio), Le and Ze, reading

$$\Lambda/L_D = \frac{\sigma}{\sigma-1}\int_1^{\sigma}\frac{\eta(\tau)}{\tau}d\tau + \frac{Ze(Le_{\text{eff}}-1)}{2(\sigma-1)}\times\int_1^{\sigma}\frac{\eta(\tau)}{\tau}\ln\left(\frac{\sigma-1}{\tau-1}\right)d\tau \qquad (1)$$

where the function $\eta(T/T_u)$ summarizes the temperature dependence of transport coefficients and Le_{eff} is an effective Lewis number which is an average of the reactants' Lewis numbers but for off-stoichiometric mixtures coincides with the Lewis number of the deficient reactant. Note that when constant properties are assumed across the flame then η ≡ 1. This model is referred to here as MCB.

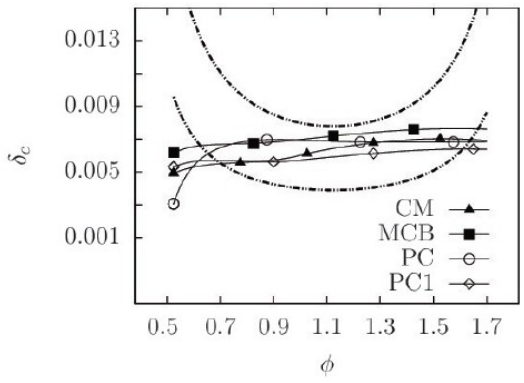

Figure 1: Critical nondimensional flame thickness δ_c *vs* equivalence ratio φ for propane/air mixtures, using different dispersion relation models. Dashed curves represent the nondimensional flame thickness $\delta = L_D/L$ for two Bunsen diameters: L=18 mm (lower dash-dotted curve) and L=9 mm (upper dash-dotted curve).

Utilizing a slightly simplified hydrodynamic flame model, in which diffusive effects are retained only in the flame speed expression, it was shown in [13] (and referred here to as CM) that a closed form dispersion relation can be derived yielding very similar results to more complete models. In particular by enforcing the dispersion relation ω = 0, an expression for the cutoff wavelength is derived, $\lambda_c = 2\pi L\,(3\sigma - 1)/(\sigma - 1)$, so that the flame is hydrodynamically unstable to any perturbation of wavelength λ such that $\lambda_c < \lambda < L$. Equivalently, the instability condition $\lambda_c < L$, dividing by L_D, translates into $\delta < \delta_c$ where $\delta_c = L_D/\lambda_c$. Thus

planar flames exhibiting nondimensional thickness smaller than the critical value δ_c are hydrodynamically unstable. This concept holds unaltered for slot flames for which the diameter L represents the minimum hydrodynamic length. Note, therefore, that DL instabilities can be induced by decreasing the thickness of the flame relative to the hydrodynamic length L. This can be accomplished by increasing the operative pressure, driving the composition towards stoichiometry or simply by increasing L.
Additional models were used, such as the one formulated by Pelce and Clavin [16], which we refer to as PC. Finally the PC model was used similarly to Ref. [20] using Eq.(1) for the Markstein length to generalize the temperature dependence. We refer to the latter model as PC1.
Regardless of the model used, to estimate δ_c by dispersion relation, we need first to know all the relevant operative parameters from the equivalence ratio, namely $\sigma(\varphi)$, $S_{0L}(\varphi)$ and $T_{ad}(\varphi)$. To this purpose we fit experimental data by Tseng et al. [21] for propane/air mixtures at atmospheric pressure. Figure (1) displays the critical flame thickness δ_c as a function of the equivalence ratio φ as estimated by the foregoing models. All models seem to yield similar results, with only a slight variability with φ, around the average value $\delta_c \approx 0.006$. As mentioned, this value acts as a guideline for the choice of the Bunsen diameters. In other words, given the flame thickness dependence on equivalence ratio for propane/air mixtures at atmospheric pressure, lD(φ), the Bunsen diameter L is chosen so that in order to trigger DL instabilities $\delta(\varphi) = L_D(\varphi)/L < \delta_c \approx 0.006$ in the range of φ of interest, and otherwise if instabilities are to be suppressed. This analysis yields a “large” diameter, chosen as L = 18 mm, for which $\delta(\varphi) < \delta_c$, at least in a wide range of near-stoichiometric mixtures which, observing Fig. 1, can be roughly estimated as φ = [0.7, 1.6]. Thus, such diameter is expected to be larger than the cutoff wavelength and therefore to exhibit DL instabilities. A “small” diameter L = 9 mm is also identified, for which $\delta(\varphi) > \delta_c$ for all values of φ, which is systematically smaller than the estimated cut-off wavelength at each φ and thus expected to be unable to sustain instabilities.
In a previous experimental study [22] the presence of DL instability was conjectured based on similar considerations and on flame curvature albeit using a single Bunsen diameter. The use of the additional smaller diameter, which is expected to suppress instabilities, is intended here to serve the purpose of unambiguously highlighting morphological differences between stable and unstable flames [15].

Experimental results

The experimental setup is similar to that described in [22, 23, 24]. As mentioned, two Bunsen diameters are utilized and the ensuing flames analyzed by means of a PIV setup using a laser source of 54 mJ Nd:YAG equipped with a 60 mm focal length camera working at a resolution of 1024×1280 pixels. The range of composition and bulk Reynolds numbers tested is reported in Table 1, where $Re = 4m/(\mu\pi L)$ with m the reactive mixture flow rate and μ the dynamic viscosity. The flame front position is determined from the sudden jump in alumina particle number density caused by the flame zone expansion which, in Mie scattering images, corresponds to zones at very different levels of scattered light intensity. Thus an intensity threshold easily identifies the flame surface. Image post processing yields global quantities such as flame surface area A_0 (under the hypothesis of axis-symmetric flame) and local quantities such as flame curvature. Thus, turbulent burning velocities, defined as the global consumption speed $S_{T,\,GC}$ recovered from $m=\rho_u S_{T,GC} A_0$, are easily recovered from the average flame front position while morphological properties can be extracted from the p.d.f.’s of curvature [22].

$L[\mathrm{mm}]$	ϕ	Re
$9.0, 18.0$	$0.7 - 1.8$	$2500 - 7000$

Table 1: Main parameters used in the experimental investigation of C_3H_8 /Air flames at atmospheric pressure.

Figure 2 shows the different morphological features of two sets of flames obtained with the two different Bunsen diameters L = 18 and 9 mm at the same Reynolds number and for the same range of equivalence ratios. In particular, signature effects due to DL instability are visible for the larger diameter in terms of cusp-like wrinkling, while these effects are absent for the smaller diameter. We now monitor the instability marker identified as the skewness of the flame curvature p.d.f.. This is shown in Fig. 3 as a function of δ/δ_c where δ_c is estimated with the CM model of Fig. 1 (albeit no significant difference is noticed using other models). We observe a clearly distinct behavior of curvature skewness depending on whether $\delta/\delta_c > 1$ or < 1. Skewness levels are related to the largest absolute curvature that can be evaluated, which, for experiments, is limited to the image resolution of 90 μm and to flame thickness which varies in the range 50 − 100 μm. Note that for each Bunsen diameter, data points on the iso-Re curves are obtained by varying the equivalence ratio φ. In particular, for the smaller diameter, data are confined to $\delta/\delta_c > 1$ and curvature skewness, which is only

mildly negative, seems to be insensitive to variations of equivalence ratio. This behavior is coherent with the absence of DL instabilities. On the other hand, for the larger diameter, data are almost entirely confined to $\delta/\delta_c < 1$ and the skewness becomes abruptly negative and highly sensitive to variations of equivalence ratio,

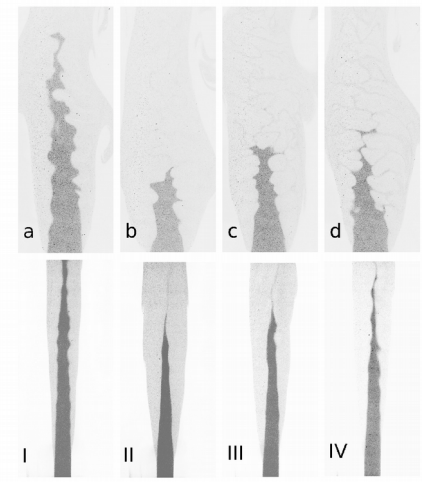

Figure 2: Mie scattering images of C3H8/Air flames at Re = 5000. Upper panels: Bunsen diameter L = 18 mm. Lower panels: L = 9 mm. Flames a-d and I-IV correspond to φ = 0.8, 1.1, 1.4, 1.5 respectively.

a behavior coherent with the presence of DL-induced morphology. This confirms, in an experimental setting, the dichotomic behavior of flame morphology with respect to variations of the parameter δ.

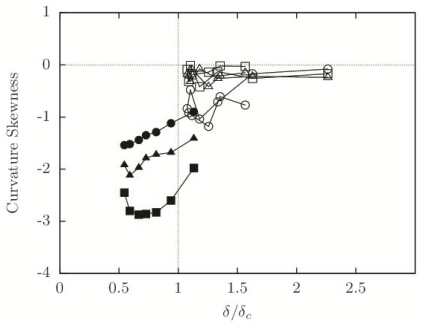

Figure 3: Skewness of flame curvature versus δ/δc for experimental C_3H_8/Air flames at Re = 2500 − 7000 using two Bunsen diameters L = 9 and 18 mm. Range of equivalence ratio for both diameters is φ = [1.1,1.7]. Squares, Re = 2500; triangles, Re = 5000; circles, Re = 7000. Open symbols represent small bunsen diameter, while filled symbols stand for large diameter.

Observing Fig. 3 and following the data sets for increasing Re numbers, we also observe a decrease in the abrupt drop in curvature skewness as $\delta/\delta_c < 1$ for higher Reynolds numbers. Thus, higher intensity translates to a reduced sensitivity of skewness to δ. This is particularly evident for the Re = 7000 data set of Fig. 3, corresponding to the highest turbulent intensity examined, for which skewness does not seem to exhibit a sudden drop as δ/δ_c is decreased below unity, but rather it seems to be subject to a uniform decrease.

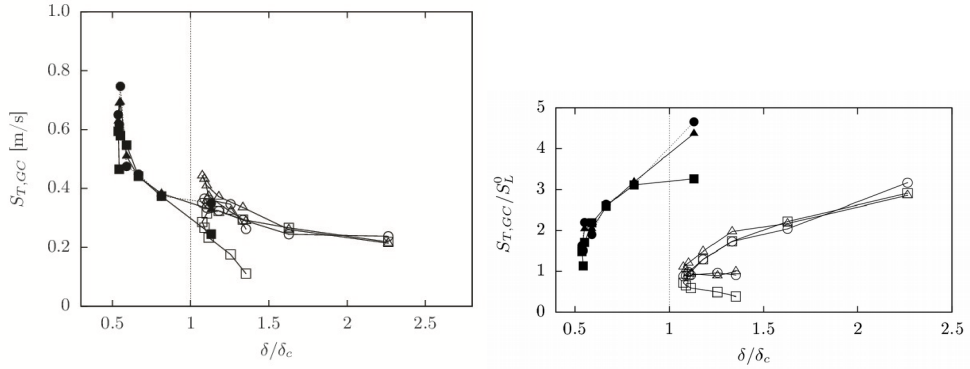

Figure 4: Left panel: turbulent burning velocity versus δ/δc for experimental C_3H_8/Air flames at Re = 2500 − 7000 using two Bunsen diameters L = 9 and 18 mm. For symbols reference, see caption of figure 3. Right panel: Turbulent

burning velocity normalized with laminar flame speed versus δ/δc. Notation is identical to Fig. 3 and 4.

Finally, for the same experimental data sets, in Fig. 4, left panel, we monitor the dimensional turbulent burning velocity S_T, evaluated as the global consumption speed $S_{T,\,GC}$ ($m=\rho_u S_{T,GC} A_0$). We observe two different regimes of turbulent propagation. While for $\delta > \delta_c$ the turbulent propagation speed seems to be rather insensitive to variations of δ, for $\delta < \delta_c$, corresponding to the larger Bunsen diameter, a DL-driven regime ensues for which the turbulent propagation speed becomes highly sensitive to δ. Indeed, Fig. 4 suggests that the presence of DL-induced flame corrugation can more than double the turbulent propa- gation speed at a given Reynolds number and mixture composition. The right panel of same figure displays the turbulent flame speed adequately rescaled with respect to the laminar flame speed. We observe a similar behavior between $\delta > \delta_c$ and $\delta < \delta_c$ with a clear amplification of the rescaled turbulent speed when $\delta < \delta_c$.

Summary

In this investigation we performed experiments of C_3H_8/Air turbulent Bunsen flames with the aim of analyzing the effects of Darrieus- Landau (DL) instability on the morphology and propagation of turbulent premixed flames.

The bifurcation parameter δ_c is estimated by adapting several analytical asymptotic models to propane/Air mixtures. DL instability is then triggered by adopting two Bunsen diameters and concurrently varying the equivalence ratio. Experimental flames exhibit a clear dichotomic behavior of flame morphology, with the curvature skewness becoming extremely sensitive to variations of δ when $\delta < \delta_c$ while remaining insensitive to δ for $\delta > \delta_c$. A similar dual behavior and enhanced sensitivity is also observed in terms of the turbulent propagation speed. In addition, Reynolds number effects, connected to turbulence intensity effects, are also analyzed. While the sensitivity to δ of curvature skewness is observed to decrease with Re, no appreciable effect is observed for the turbulent propagation speed.

References

[1] P.Cambray, G. Joulin, Proc. Combust. Inst. 24 (1992) 61–67.
[2] H. Kobayashi, T. Tamura, K. Maruta, T. Niioka, Proc. Comb. Inst. 26 (1996) 389–396.
[3] R. Paul, K. Bray, Proc. Comb. Inst. 26 (1996) 259–266.
[4] H. Kobayashi, Y. Kawabata, K. Maruta, Proc. Comb. Inst. 27 (1998) 941–948.
[5] H. Kobayashi, H. Kawazoe, Proc. Comb. Inst. 28 (2000) 375– 381.
[6] V. Savarianandam, C. Lawn, Combustion and Flame 146 (2006) 1–18.
[7] A. Al.Shahrany, D. Bradley, M. Lawes, K. Liu, R. Woolley, Combust. Sci. and Tech. 178 (2006) 1771–1802.
[8] D. Bradley, M. Lawes, L. Kexin, M. Mansour, Proc. Comb. Inst.34 (2013) 1519–1526.
[9] M. Matalon, F. Creta, Comptes Rendus-Mecanique340 (2012) 845–858.
[10] N. Fogla, F. Creta, M. Matalon, Proc. Comb. Inst. 34 (2013) 1509–1517.
[11] F. Creta, M. Matalon, J. Fluid Mech. 680 (2011) 225–264.
[12] F. Creta, N. Fogla, M. Matalon, Comb. Th. and Modelling 15 (2011) 267-298.
[13] F. Creta, M. Matalon, Proc. Comb. Inst. 33 (2011) 1087–1094.
[14] C. Clanet, G. Searby, Phys.Rev.Lett. 80 (1998) 3867–3870.
[15] F. Creta, R . Lamioni, P.E. Lapenna, G. Troiani, Physical Review E 94 (2016) 053102.
[16] P. Pelce, P. Clavin, J. Fluid Mech. 124 (1982) 219–237.
[17] M. Matalon, B. Matkowsky, J. Fluid. Mech. 128 (1982) 239–259.
[18] M. Frankel, G. Sivashinsky, Combust. Sci. Technol. 29 (1982) 207–224.
[19] M. Matalon, C. Cui, J. Bechtold, J. Fluid. Mech. 487 (2003) 179– 210.
[20] S. Chaudhuri, V. Akkerman, C. Law, Phys. Rev. E 84 (2011) 026322.
[21] L. K. Tseng, M. A. Ismail, G. M. Faeth, Combust. Flame 95 (1993) 410–426.
[22] G. Troiani, F. Creta, M. Matalon, Proc. Comb. Inst. 35 (2015).
[23] F. Picano, F. Battista, G. Troiani, C. M. Casciola, Experiments in Fluids 50 (2011) 75–88.
[24] G. Troiani, M. Marrocco, S. Giammartini, C. M. Casciola, Combust. Flame 156 (2009) 608–620.